JCTC Journal of Chemical Theory and Computation

Inductive and External Electric Field Effects in Pentacoordinated Phosphorus Compounds

Enrique Marcos, Ramon Crehuet,* and Josep M. Anglada*

Grup de Química Teòrica i Computacional, Departament de Química Orgànica Biològica, Institut d'Investigacions Químiques i Ambientals de Barcelona, IIQAB − CSIC, c/ Jordi Girona 18, E-08034 Barcelona, Spain

Received August 28, 2007

Abstract: Pentacoordination at phosphorus is associated with a nucleophilic displacement reaction at tetracoordinated phosphorus compounds and shows a great variability in what respects their geometrical and energetic features. By means of a systematic theoretical study on a series of elementary model compounds, we have analyzed the bonding features. The pentacoordinated phosphorus compounds are held together by dative bonds, and the geometry and stability depends on the inductive effects originated by different substitutes at phosphorus. We show also that an external electric field can modify the geometrical features and the reactivity of the nucleophilic substitution reactions. This issue may have great interest in biological reactions involving pentacoordinated phosphorus where the electric field originated by the folded protein could influence the catalytic process. We report also additional calculations on the geometry and NMR spectra on three triphenyl phosphonium ylide derivatives, and our results compare well with the experimental data.

Introduction

A detailed knowledge on the electronic nature of pentacoordination at phosphorus is of great interest in chemistry and biochemistry.[1−12] Pentacoordination at phosphorus is mainly associated with a nucleophilic displacement reaction at tetracoordinated phosphorus compounds, which is associated with cell signaling and energetics and many aspects of biosynthesis. These nucleophilic reactions occur in the so-called associative processes, which can follow a concerted pathway, with a trigonal bipyramid transition state, or an addition−elimination pathway, involving a pentacoordinated phosphorane intermediate.[7−9,11,13,14] These processes are important in chiral reactions. Those following a concerted pathway take place with inversion of configuration, but in pathways involving pentacoordinate intermediates, a Berry pseudorotation may occur, which could involve retention of configuration.[5,11] Pentacoordinated phosphorus intermediates are found, for instance, in the Wittig reaction,[15] in human α-thrombin inhibitors,[1] and as intermediates in the hydrolysis of phospholipids catalyzed by phospholipase D.[6] It may exist in phosphoryl transfer in GTP hydrolysis by RAS proteins[10] and as an intermediate in the phosphoryl transfer reaction catalyzed by a β-phosphoglucomutase,[2,16] although some controversy exists in the literature regarding the true nature of this intermediate.[3,4]

Pentacoordination at phosphorus occurs mainly in trigonal bipyramid structures, and it has been observed that the apical bond lengths show a great variability, which depends on several factors as the nature of the substitutes at P, the influence of hydrogen bonding or the charge around phosphorus.[1,10,11,17,18] It appears therefore that such variability would affect not only the stability of these compounds but also the transition states involving pentacoordination at phosphorus and consequently the reactivity. The factors affecting this variability are crucial for a complete understanding of nucleophilic displacement at phosphorus. They are still not well rationalized and are the main goal of this study.

Extensive theoretical studies have also been reported in the literature, which have provided valuable information regarding different aspects of the reaction mechanisms of

* Corresponding author e-mail: anglada@iiqab.csic.es (J.M.A.), rcsqtc@iiqab.csic.es (R.C.).

10.1021/ct700220z CCC: $40.75
Published on Web 12/05/2007

phosphate reactions, the importance and possible existence of pentacoordinated intermediates depending on the reaction conditions, and the effects of the solvent in the reactivity.[19−47] In this study we have focused our attention on the inductive effects affecting pentacoordination at phosphorus and its bonding features. To this end, we have considered, in the first stage, a series of model systems for which we have investigated the effect of different substitutes at phosphorus as well as the effect of polarization and the effect of an external electric field. In the second stage, we have also investigated a series of triphenylphosphonium ylide derivatives for which experimental data exist in the literature.

Computational Details

All geometry optimizations carried out in this work have been performed with the density functional *m*PW1PW91[48] employing the 6-31+G(d) basis set.[49] At this level of theory we have also calculated the harmonic vibrational frequencies to verify the nature of the corresponding stationary point (minima or transition state) and to provide the zero point vibrational energy (ZPE). The *m*PW1PW91 functional has been found to be adequate to describe systems with long-range interactions, especially with dative bonds.[50] Moreover, the reliability of this functional, with respect to the geometrical parameters, has also been checked by performing, for some test models, comprehensive test calculations employing the MP2[51−53] ab initio approach and using the 6-31+G(d), 6-311+G(d), and 6-311+G(3df, 3pd) basis sets. The results obtained compare quite well and are collected in the Supporting Information. Moreover, for the cases where reactivity has been considered, we have performed, for each transition state, intrinsic reaction coordinate calculations (IRC)[54−56] in order to ensure that the transition states connect the desired reactants and products. In the second step, the relative energies of the stationary points were corrected by performing single point energy calculations using the *m*PW1PW91 functional with the 6-311+G(3df,2p) basis set.[57] In addition, we have also checked the reliability of the activation and reaction energies by performing, for all stationary points of a given reaction (reaction **1b**, see below), additional single point energy calculations at the higher level of theory CCSD(T)/IB.[58−62] The results obtained at the *m*PW1PW91 and CCSD(T) level compare very well and are contained in the Supporting Information.

For the three triphenylphosphonium ylides considered, we have also computed the NMR spectra by performing B3LYP single-point calculations[63] at the optimized geometries, using the GIO method[64,65] and employing the 6-311+G(2d,p) basis set.[57]

The quantum chemical calculations carried out in this work were performed by using the Gaussian[66] program package, and the Molden program[67] was employed to visualize the geometric and electronic features.

The bonding features of the different systems considered were analyzed by employing the natural bond orbital (NBO) partition scheme by Weinhold and co-workers[68] and the atoms in molecules (AIM) theory by Bader.[69] The topological properties of wave functions were computed using the AIMPAC program package.[70]

Scheme 1 [a]

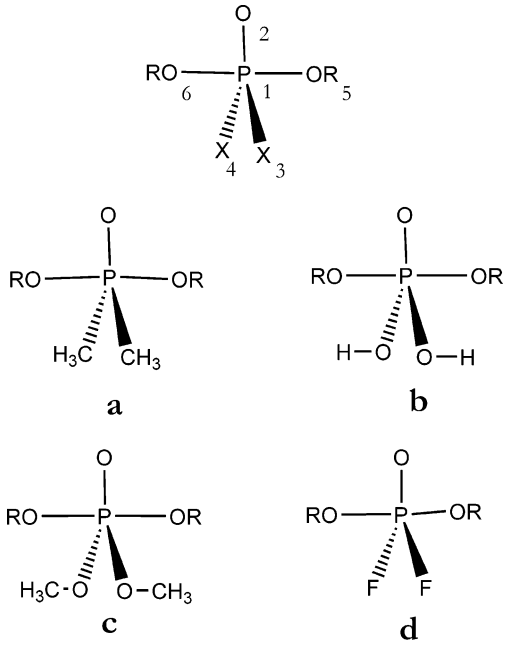

[a] RO = HO (**1**); CH_3O (**2**); HCOO (**3**); CF_3O (4).

Results and Discussion

The Model Systems $POX_2(RO)_2$ Pentacoordinated Compounds. One important point regarding the chemistry of pentacoordinated phosphorus compounds refers to the variability of the apical bond distances.[5,11] In order to analyze and rationalize this issue we have carried out a series of calculations on the $POX_2(RO)_2$ model systems. These pentacoordinated model systems have been depicted in Scheme 1 and possess a trigonal bipyramid structure. Here X are equatorial substitutes (X = CH_3 (**a**); HO (**b**); CH_3O (**c**); and F (**d**)) and RO are apical substitutes (RO = HO (**1**); CH_3O (**2**); HCOO (**3**); and CF_3O (**4**)). Along this work, the different models are labeled by a number as a prefix, according to the apical substitutes, followed by a letter as a suffix according to the equatorial substitutes. Thus, compound **1a** corresponds to $PO(CH_3)_2(OH)_2$, whereas compound **3c** corresponds to $PO(CH_3O)_2(HCOO)_2$ (see Scheme 1).

Please note also that in these model systems the charge of the system is −1, the two apical substitutes are identical, and that in **b** and **c** the two equatorial substitutes are oppositely oriented. Moreover, it is also worth reminding the reader that the donor character of the apical substitutes is HO > CH_3O > HCOO > CF_3O and the donor character of the equatorial substitutes is CH_3 > HO > CH_3O > F so that these series of model systems allow us to analyze combinations of electron withdrawing groups and electron donor groups on the phosphorus coordination. The most significant geometrical parameters of the optimized structures are displayed in Table 1, which also includes the tetracoordinated phosphoric acid H_3PO_4 for comparison. Figure 1 shows the dependence of the apical bond lengths with respect to the apical and equatorial substitutes at P. The Cartesian coordinates of each pentacoordinated model system are reported in the Supporting Information.

For H_3PO_4, Table 1 shows that our calculations predict the P···O bond length to be 1.476 Å and the three P···OH

Table 1. Optimized Bond Lengths (in Å) to Phosphorus in H_3PO_4 and the Pentacoordinated **1a**−**4d** Model Compounds

	substitutes				
compd	apical	equatorial	r(P−OR$_{apical}$)	r(P−X$_{equatorial}$)	r(P−O)
H_3PO_4				1.602	1.476
1a	OH	CH_3	1.814	1.849	1.545
1b	OH	OH	1.768	1.660	1.527
1c	OH	OCH_3	1.742	1.673	1.539
2a	OCH_3	CH_3	1.841	1.841	1.521
2b	OCH_3	OH	1.778	1.660	1.510
2c	OCH_3	CH_3	1.749	1.677	1.514
3a	OC(H)O	CH_3	1.908	1.832	1.507
3b	OC(H)O	OH	1.835	1.635	1.495
3c	OC(H)O	OCH_3	1.818	1.639	1.499
3d	OC(H)O	F	1.780	1.609	1.496
4a	OCF_3	CH_3	1.980	1.826	1.488
4b	OCF_3	OH	1.878	1.625	1.480
4c	OCF_3	OCH_3	1.882	1.616	1.484
4d	OCF_3	F	1.808	1.591	1.476

bond lengths to be 1.602 Å. The nucleophilic addition of the HO anion to H_3PO_4 leads to the pentacoordinated compound **1b** and produces a lengthening of 0.051 Å in the P···O bond and of 0.058 Å in the equatorial P···OH bonds, compared with the P···O and the P···OH bond lengths in phosphoric acid, but the two apical P···OH bond distances (1.768 Å) are predicted to be much longer (see Table 1).

Regarding the remaining pentacoordinated model systems, the results of Table 1 and Figure 1 show a great variability of the P···OR$_{apical}$ bond length, which depends on the character of both X and RO. Thus, the apical bond distance changes as much as 0.238 Å, from 1.742 Å in **1c** to 1.980 Å in **4a**, whereas the changes in the equatorial bond lengths (P···X$_{equatorial}$ and P···O$_{equatorial}$) are smaller than 0.070 Å for all the model compounds. Table 1 and Figure 1 also show that, for the same equatorial substitute, the P···OR$_{apical}$ bond length is shorter as the donor character of OR increases, while the donor character of the equatorial substitute X results in an increase of the P···OR$_{apical}$ bond length. Thus, for instance, for X = CH_3, the P···O$_{apical}$ bond distance changes from 1.814 Å in **1a** (apical substitute = OH) to 1.980 Å in **4a** (apical substitute = OCF_3), while for X = CH_3O, the P···O$_{apical}$ bond distance changes from 1.742 Å in **1c** (apical

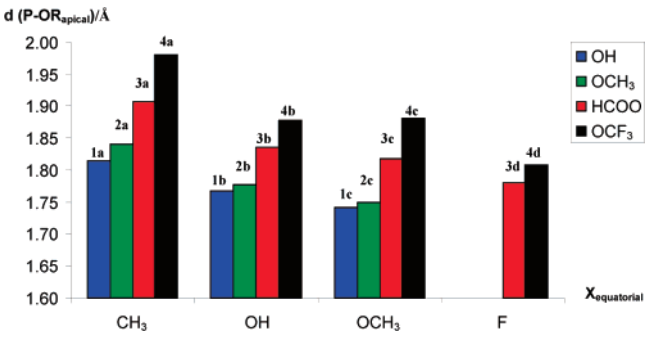

Figure 1. Diagram showing the dependence of the apical bond lengths in the pentacoordinated $POX_2(RO)_2$ model compounds on the nature of the apical (RO) and equatorial (X) substitutes on P.

Table 2. Natural Occupation at Phosphorus, Stabilization Energies ($\Delta E(2)$ in kcal·mol^{-1}) Associated with the Most Important Donor−Acceptor Interaction Involving the Apical Bonds and the Natural Charges at Phosphorus (Q in e)[d]

	P natural occupation			stabilization energies			
compd	s	p	d	$\sigma_{P1O5} \rightarrow \sigma^*_{P1O6}$ [a]	$\sigma_{P1X} \rightarrow \sigma^*_{P1O6}$ [b]	$\sigma_{P1O2} \rightarrow \sigma^*_{P1O6}$ [c]	Q_{NBO}(P)
1a	0.91	1.85	0.09	33.51	30.67	28.88	2.12
1b	0.77	1.59	0.11	29.80	22.66	21.59	2.51
1c	0.77	1.56	0.11	28.86	20.02	23.54	2.54
2a	0.91	1.81	0.08	31.86	39.14	27.90	2.17
2b	0.77	1.55	0.10	25.50	30.71	20.28	2.56
2c	0.76	1.51	0.10	24.27	24.41	16.98	2.59
3a	0.94	1.82	0.08	35.52	35.23	31.58	2.13
3b	0.77	1.57	0.10	29.04	24.04	23.34	2.53
3c	0.77	1.53	0.10	28.80	24.08	22.12	2.58
3d	0.76	1.49	0.11	24.88	20.59	24.90	2.62
4a	0.95	1.82	0.07	35.94	38.97	34.06	2.12
4b	0.77	1.57	0.10	29.43	24.43	26.59	2.53
4c	0.77	1.53	0.10	32.39	25.32	27.89	2.58
4d	0.75	1.50	0.11	28.48	22.90	28.43	2.62

[a] $\sigma_{P1O5} \rightarrow \sigma^*_{P1O6}$has the same value as $\sigma_{P1O6} \rightarrow \sigma^*_{P1O5}$. [b] The same interaction occurs from each σ_{PX} equatorial to each σ^*_{PO} apical bond. [c] $\sigma_{P1O2} \rightarrow \sigma^*_{P1O6}$has the same value as $\sigma_{P1O2} \rightarrow \sigma^*_{P1O5}$. [d] Bond numbering is according Scheme 1.

substitute = OH) to 1.883 Å in **4c** (apical substitute = OCF_3) (see Table 1 and Figure 1). In the case whether the equatorial substitute X is F, we have only found pentacoordinated compounds with apical substitutes HCOO (**3d**) and CF_3O (**4d**).

These results indicate two important points, namely a different nature of the apical and equatorial bonds and a great importance of inductive effects on pentacoordinated phosphorus compounds. In order to get a deeper knowledge of the features of bonding at phosphorus, we have carried out a study of the bond properties according to the Atoms in Molecules (AIM) theory by Bader and the Natural Bond Orbital (NBO) theory by Weinhold. A detailed discussion of the AIM analysis is given in the Supporting Information along with the computed topological parameters at the bcp of the P···O$_{apical}$, the P···X$_{equatorial}$, and the P···O bonds collected in Table S4. In general, and regarding the apical bonds, the range of values for ρ_b and $\nabla^2\rho_b$ are characteristic of "closed shell" interactions, so that *the two apical bonds in these model systems can be classified as dative*. The large variability of the P···O apical bonds pointed out above, depending on the nature of the substitutes, is also typical of dative interactions.[71,72]

Additional information is provided by the NBO analysis. In Table 2 we have displayed the natural occupation at the P atom, the natural charge on P, and the stabilization energies ($\Delta E(2)$) associated with the charge-transfer interactions of the relevant donor−acceptor orbitals involving the apical bonds, that is, the bonding σ(P−O$_{apical}$), σ(P−X$_{equatorial}$), and σ(P−O) NBOs with the antibonding acceptor σ^*(P−O$_{apical}$) NBO. This stabilization energy has been computed with the second-order perturbation theory with the Fock matrix in the NBO analysis and the natural charges on phosphorus. The NBO analysis indicates that the natural occupation in the d

shell is always less than or equal to 0.11 and consequently *excludes the participation of the d-orbital in the hybridization picture*. Thus, there is a formal sp^2 hybridization at P in all pentacoordinated model compounds. The d orbitals act as polarization functions in a similar way as pointed out by Reed and co-workers in a study on chemical bonding in hypervalent molecules[73] and in pentacoordinated silicon compounds bonded also by dative bonds.[72] This formal hybridization scheme is also compatible with the simple MO diagram based on a three-center four-electron (3c4e) model.[11,74] Another important point to be mentioned here refers to the topological features of the NBO orbitals linked to phosphorus. Those NBO orbitals designed as bonding orbitals of the type P···O or P···F in Table 2 are highly polarized toward the O or F atom, whereas those designed as antibonding orbitals have an almost exclusive contribution of phosphorus. Thus, the donor−acceptor interaction between these NBOs displayed in Table 2 represents quite well charge-transfer interactions. Moreover, this topological picture agrees very well with the dative description of the P···O bonds provided by the AIM analysis and discussed above. By the same way, the P···C bonds in compounds **1a**, **2a**, **3a**, and **4a** (with CH_3 as equatorial substitutes) have an almost equal contribution of phosphorus and carbon, according to the covalent character predicted by the AIM analysis (see above). The most important perturbative donor−acceptor interactions involving the equatorial substitutes ($\sigma_{PX-equatorial} \rightarrow \sigma^*_{PO-apical}$) are those having X = CH_3 (compounds **1a**, **2a**, **3a**, and **4a**) according to the well-known donor character of the methyl substitute and decreases according to the donor character of the equatorial substitutes (see above). Also very interesting are the perturbative donor−acceptor interactions between the two apical bonds ($\sigma_{P1O5} \rightarrow \sigma^*_{P1O6}$) and ($\sigma_{P1O6} \rightarrow \sigma^*_{P1O5}$) that involve charge transfer between the two apical bonds. Here it is also worth pointing out that these apical donor−acceptor interactions are symmetrical because the two apical groups are the same (see footnote b of Table 2). However, as will be shown below, when the two apical groups are different, the two apical donor−acceptor interactions are different, pointing out the competition of these two groups to form a dative bond to phosphorus and therefore having a direct influence on the corresponding P···O bonds.

Nucleophilic Substitution on the Model $POX_2(OR)_2$ Pentacoordinated Compounds. A very important point concerning the pentacoordinated $POX_2(OR)_2$ compounds discussed above refers to their relative stability. This has been studied in connection with the formation via a S_N2 reaction according to eq 1.

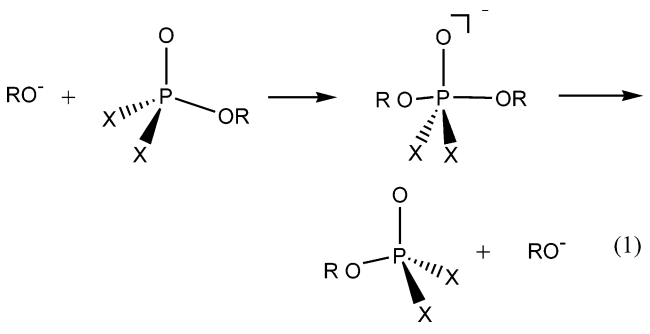

(1)

Please note that in this section, all reactions considered are symmetric as the entrance and leaving groups are identical. Each reaction described by eq 1 has been named according to the substitutes in the same way as has been done in the previous section to characterize the pentacoordinated phosphorus model compounds as displayed in Scheme 1. Thus, for instance, reaction **1a** means $RO^- = HO^-$ and X = CH_3, or reaction **4c** means RO = CF_3O^- and X = OCH_3; that is, each reaction has the same name that identifies the pentacoordinated intermediate. A schematic representation of the corresponding potential energy surfaces has been drawn in Figures 2 and 3, whereas the geometric parameters of the corresponding stationary points are collected in the Supporting Information. The energetic of these processes is contained in Table 3.

Figure 2a shows a schematic potential energy profile of reactions **1a**−**4a**, having the CH_3 group as equatorial substitute X. Each reaction begins with the formation of a prereactive hydrogen-bonded complex which occurs previous to the transition state and the formation of the pentacoordinate intermediate. Every prereactive complex has two hydrogen bonds, which occur between the oxygen of the anion (RO^-) and one of the hydrogen atoms of each equatorial methyl substitute. For reaction **3a** (red line, having HCOO as apical substitutes), the two hydrogen bonds in the prereactive complex are formed between each one of the oxygen atoms of the HCOO anion and one of the hydrogen atoms of each equatorial methyl substitute. The stability of these hydrogen-bonded complexes at 0 K is computed to vary among 24.3 and 16.6 kcal·mol^{-1} (for reactions **1a**−**4a**, see Table 3), and these energy values in gas phase are typical of hydrogen bond interactions involving an anion. After surmounting an energy barrier of the order of 5−6 kcal·mol^{-1}, the corresponding pentacoordinate intermediate is formed, and its stability, at 0 K, is computed to be among 33.1 and 15.9 kcal·mol^{-1}, relative to RO^- plus $POX_2(OR)$. The stability in these intermediates depends on the donor character of the apical substitutes. There is a large difference in the relative stability of the **1a** (blue line, apical substitute HO) and the stability of **4a** (black line, with apical substitute CF_3O), which amounts 16 kcal·mol^{-1}, so that *the compounds having the apical substitute with higher donor character are more stable.* This higher stability is associated with shorter apical bond lengths as discussed in the previous section for compounds **1a**, **2a**, **3a**, and **4a**.

In the case of the two equatorial (Figure 2b) substitutes X is the F atom, and we have only considered the reaction with $RO^- = HCOO^-$ (**3d**) and $RO^- = CF_3O^-$ (**4d**), since these are the only ones in which the F substitutes remain in the equatorial position as pointed out in the previous section. Both reactions occur by direct formation of a pentacoordinated phosphorus compound, whose stability at 0 K has been computed to be 32.1 and 20.7 kcal·mol^{-1}, for **3d** (red line) and **4d** (black line), respectively, according also to the higher donor character of the apical substitute in **3d** (see also Table 3). The processes are similar to those described recently by van Bochove and co-workers[24] in a recent study on nucleophilic substitution at phosphorus having fluorine atoms as equatorial substitute.

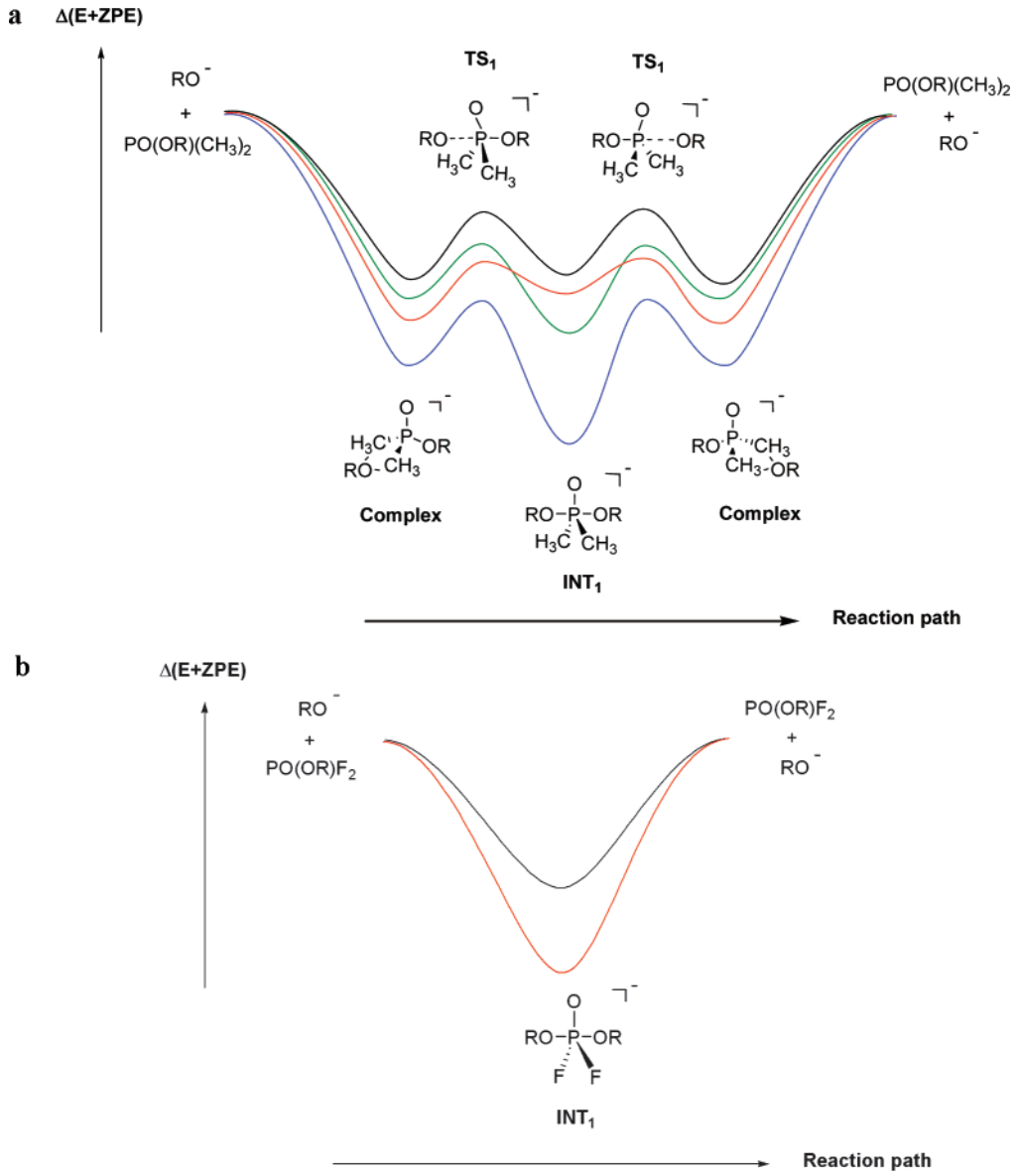

Figure 2. Schematic potential energy diagram for the nucleophilic substitution reactions: In (a), $RO^- + PO(OR)(CH_3)_2 \rightarrow PO(OR)(CH_3)_2 + RO^-$: (RO = HO, blue line; CH_3O, green line; HCOO, red line; and CF_3O, black line). In (b), $RO^- + PO(OR)(F)_2 \rightarrow PO(OR)(F)_2 + RO^-$: (RO = HCOO, red line; CF_3O, black line). The relative energies are computed at the *m*PW1PW91/6-311+G(3df,2p)//*m*PW1PW91/6-31+G(d) level of theory.

For the equatorial substitute X = OH, namely reactions **1b**−**4b**, the precursors of the corresponding pentacoordinated phosphorus compound are not RO^- and $PO(OH)_2OR$ as described in eq 1, but its respective conjugate acid (ROH) and basis ($PO(OH)(O)OR^-$), which occurs because $PO(OH)_2OR$ is a stronger acid than H_2O, CH_3OH, HCOOH, and CF_3OH, respectively (among 13.3 and 64.6 kcal·mol^{-1}, see reactions **1b**−**4b** in Table 3). Therefore, these model reactions involve a proton transfer linked to the formation of a pentacoordinated phosphorus compound, in a similar way as many reactions of biological interest. The schematic reaction profiles are depicted in Figure 3a, which shows that the reaction begins with the formation of a hydrogen-bonded complex which occurs previous to the formation of the pentacoordinated intermediate. This is a concerted process where the proton transfer from ROH to $PO(OH)(O)OR^-$ takes place simultaneously to the addition of the RO group to phosphorus. The results displayed in Table 3 and Figure 3a show that the computed stability of the prereactive hydrogen-bonded complexes ranges among 12.7 and 27.2 kcal·mol^{-1} and that the barrier that has to be overcome to form the pentacoordinated intermediate ranges among 37.1 and 27.5 kcal·mol^{-1} for **1b**−**4b**, respectively. Table 3 and Figure 3a show that all pentacoordinated intermediates lie energetically above the reactants (among 17 and −0.4 kcal·mol^{-1}). This reaction mechanism and the corresponding energetic profile is comparable to that of the dimethylphosphate hydrolysis and the ethylene phosphate hydrolysis reported recently.[26,28]

The last model reactions we have considered are those having X = CH_3O as equatorial substitutes and correspond to reactions **1c**−**4c**. A look at the schematic energy profile in Figure 3b shows that, for **1c**, **2c**, and **3c** (blue, green, and red lines respectively), the reaction has a 5-fold well. As

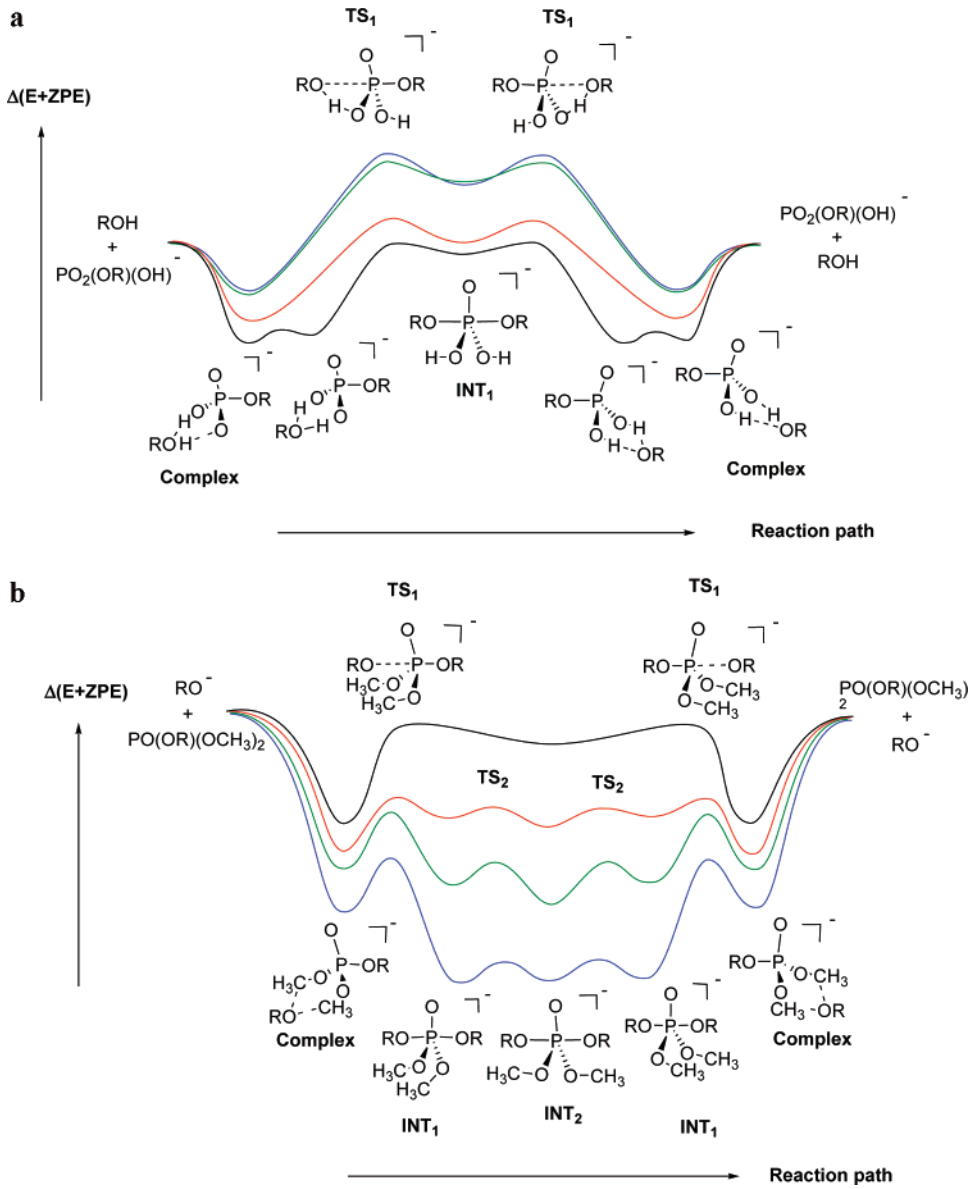

Figure 3. Schematic potential energy profiles for the nucleophilic substitution reactions: $RO^- + PO(OR)(X)_2 \rightarrow PO(OR)(X)_2 + RO^-$: (RO = HO, blue line; CH_3O, green line; HCOO, red line; and CF_3O, black line) in (a) X = (HO) and in (b) X = (CH_3O). The relative energies are computed at the *m*PW1PW91/6-311+G(3df,2p)//*m*PW1PW91/6-31+G(d) level of theory.

before, the reactions begin with the formation of a pentacoordinated hydrogen-bonded complex (first minimum), while the second, third, and fourth minima correspond to the pentacoordinated intermediates with the OCH_3 equatorial substitutes having different orientations, namely parallel to the side of the reactants (**INT1**), opposite (**INT2**), and parallel to the side of the products (**INT1**). The occurrence of similar multiple transition states separating the pentacoordinated species from the precursor complexes has been reported recently by van Bochove and co-workers,[24] who addressed this phenomenon to the increased steric bulk. For **4c** (black line) only one pentacoordinated intermediate has been found (**INT2**), being that the CH_3O equatorial substitutes are oppositely oriented. A more detailed discussion on these different conformers of the pentacoordinated phosphorus compounds will be given in the next section, and, for the aim of this section, it is only worth remarking here that the stability of the two pentacoordinated conformers differ only at most by 3 kcal·mol^{-1} (see Table 3). The results displayed in Table 3 reveal that the prereactive hydrogen-bonded complexes are computed to be among 26 and 15 kcal·mol^{-1} more stable than the reactants, and the formation of the pentacoordinated intermediate requires to surmount an energy barrier of among 7 and 12 kcal·mol^{-1}. Moreover, the stability of the pentacoordinated phosphorus intermediates follows the same trends as discussed above, namely that the intermediates having apical substitutes with higher donor character are more stable. That is 35.7 kcal·mol^{-1} for **1c** (apical substitute HO); 25.4 kcal·mol^{-1} for **2c** (apical substitute CH_3O); 15.2 kcal·mol^{-1} for **3c** (apical substitute HCOO); and 3.5 kcal·mol^{-1} for **4c** (apical substitute CF_3O). In addition, it is also worth mentioning that, as shown in Table 3, in the case of **1c** and **2c** (having apical substitutes with a large donor character) the pentacoordinated phosphorus intermediates are considerably more stable than the

Table 3. Relative Energies ($\Delta(E+ZPE)$ in kcal·mol^{-1}) Computed at the *m*PW1PW91/6-311+G(3df,2p)// *m*PW1PW91/6-31+G(d) Level of Theory for the Nucleophilic Substitution Reactions **1a**−**4d**

reaction[a]	$RO^- + POX_2(OR)$	$ROH + POX_2(OR)^-$	complex	TS1	INT1	TS2	INT2
1a	0.0		−24.3	−19.4	−33.1		
2a	0.0		−18.1	−13.3	−22.0		
3a	0.0		−20.4	−14.0	−17.9		
4a	0.0		−16.6	−9.9	−15.9		
1b	64.6	0.0	−12.7	24.4	17.2		
2b	52.4	0.0	−13.0	22.3	16.5		
3b	28.7	0.0	−18.8	5.7	1.3		
4b	13.3	0.0	−27.2	0.3	−0.4		
1c	0.0		−25.8	−18.9	−34.9	−32.7	−35.7
2c	0.0		−20.4	−13.2	−22.4	−19.9	−25.4
3c	0.0		−18.3	−11.5	−14.2	−12.7	−15.2
4c	0.0		−15.1	−2.2	−3.5		
3d	0.0				−32.1		
4d	0.0				−20.7		

[a] The following acronyms stand for the corresponding reactions: **1a** = $HO^- + OP(CH_3)_2(HO)$; **2a** = $CH_3O^- + OP(CH_3)_2(CH_3O)$; **3a** = $HCOO^- + OP(CH_3)_2(HCOO)$; **4a** = $CF_3O^- + OP(CH_3)_2(CF_3O)$; **1b** = $HO^- + OP(OH)_2(HO)$; **2b** = $CH_3O^- + OP(OH)_2(CH_3O)$; **3b** = $HCOO^- + OP(OH)_2(HCOO)$; **4b** = $CF_3O^- + OP(OH)_2(CF_3O)$; **1c** = $HO^- + OP(OCH_3)_2(HO)$; **2c** = $CH_3O^- + OP(OCH_3)_2(CH_3O)$; **3c** = $HCOO^- + OP(OCH_3)_2(HCOO)$; **4c** = $CF_3O^- + OP(OCH_3)_2(CF_3O)$; **3d** = $HCOO^- + OPF_2(HCOO)$; **4d** = $CF_3O^- + OPF_2(CF_3O)$.

prereactive hydrogen-bonded complexes, as opposed to what occurs for **3c** and **4c**.

Finally, it is also worth pointing out that the main reaction features described for these nucleophilic substitutions at phosphorus occur also in nucleophilic substitution reactions at silicon as reported by Bento and co-workers.[75]

Conformational Change in Equatorial Substitutes. The Polarization Effects. In the previous section we have pointed out that reactions **1c**−**3c** occur in several steps involving conformational changes in the orientation of the CH_3O equatorial substitutes. The corresponding energy barriers are smaller than 3.0 kcal·mol^{-1}, whereas the two conformers differ in energy at most by 3 kcal·mol^{-1} (see Table 3). Despite these small energetic differences in the two conformers, an analysis of its structures reveals significant differences with respect to the geometrical parameters concerning the apical substitutes. Therefore we have investigated the effect of the conformational changes (opposite and parallel orientation) on the equatorial substitutes in the model systems having HO and CH_3O as equatorial substitutes. In the case of the HO equatorial substitutes, only the model having HO as apical substitutes has both conformers stable (**1b** and **1b′**), whereas for the CH_3O equatorial substitutes the models with the HO, CH_3O, and HCOO apical substitutes have the two conformers stable (**1c** and **1c′**; **2c** and **2c′**; and **3c** and **3c′**; respectively). In Figure 4 we have displayed the most significant geometrical parameters of these conformers.

As pointed out in a previous section, the **1b** model has the two apical P···O(H) bond lengths equal to 1.768 Å (see Table 1). However a conformational change in the equatorial substitute leading to a parallel orientation (model **1b′**) produces an important change in the two apical P···O(H) bond lengths (1.695 and 1.910 Å, respectively); that is, the P···O apical bond length opposite to the orientation of the two equatorial OH substitutes is reduced by 0.073 Å and the other P···O apical bond length is enlarged by 0.142 Å. On the other hand, the changes in the equatorial bond lengths are very small (see Figure 4). From an energetic point of view, both conformers are separated by only 0.87 kcal·mol^{-1} ($\Delta(E + ZPE)$ value), being that **1b′** is more stable than **1b**. Looking for the origin of these differences we have first considered the possible existence of intramolecular hydrogen bond interactions that could stabilize one of these two conformers, but the AIM analysis ruled out this fact. Moreover, the NBO analysis indicates that the parallel orientation of the equatorial substitutes (structure **1b′**) induces a differential polarization effect on P, which results in a change of the phosphorus ability to bear an electronic charge and affecting therefore the axial bond length. In other words, the polarization on P produces a greater or less repulsion with the axial group (depending on the side) originating a change on the corresponding equilibrium bond distance. This polarization effect is not produced in those compounds with opposite oriented equatorial substitutes (structure **1b**) because of a cancellation effect due to the opposite orientation. For **1b**, the NBO analysis has already been reported in a previous section (see Table 2), where it has been pointed out that charge transfer occurs symmetrically. The perturbative donor−acceptor interactions involving the equatorial substitutes ($\sigma_{PO-equatorial} \rightarrow \sigma^*_{PO-apical}$) are equal to 22.6 kcal·mol^{-1} (from each of the two $\sigma_{PO-equatorial}$ to each of the two $\sigma^*_{PO-apical}$), whereas perturbative donor−acceptor interactions between the two apical bonds ($\sigma_{P1O5} \rightarrow \sigma^*_{P1O6}$ and $\sigma_{P1O6} \rightarrow \sigma^*_{P1O5}$) are both equal to 29.8 kcal·mol^{-1}. In the case of the conformer **1b′**, the situation changes radically, and the perturbative donor−acceptor interactions are not symmetrical anymore. The inductive effects, reflected in the perturbative donor−acceptor interactions involving the equatorial substitutes ($\sigma_{P1O3} \rightarrow \sigma^*_{P1O6}$ and $\sigma_{P1O4} \rightarrow \sigma^*_{P1O6}$), are 25.2 kcal·mol^{-1}, whereas ($\sigma_{P1O3} \rightarrow \sigma^*_{P1O5}$ and $\sigma_{P1O4} \rightarrow \sigma^*_{P1O5}$) are 20.5 kcal·mol^{-1}. That is, there is a greater charge transfer to the P1O6 side (σ^*_{P1O6} orbital) that affects the perturbative donor−acceptor interactions between the two apical bonds

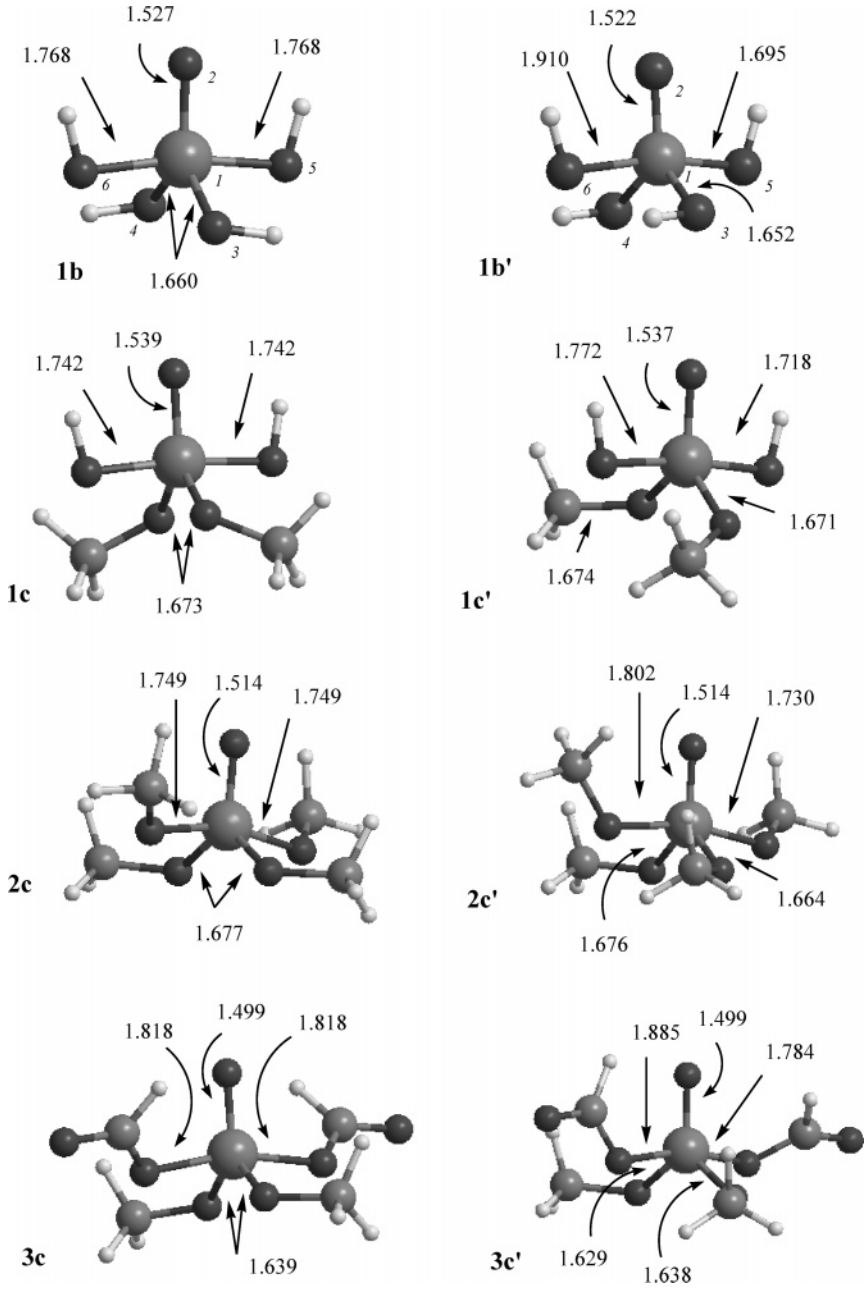

Figure 4. Selected geometrical parameters (in Å) for the optimized structures **1b**, **1b′**, **1c**, **1c′**, **2c**, **2c′**, **3c**, and **3c′**.

($\sigma_{P1O5} \rightarrow \sigma^*_{P1O6}$ = 32.1 kcal·mol^{-1} and $\sigma_{P1O6} \rightarrow \sigma^*_{P1O5}$ = 27.7 kcal·mol^{-1}), and, consequently, we can conclude that *the differential polarization effect originated by the conformational change induces a competition between the two equal apical substitutes in the pentacoordinated phosphorus compound*.

In order to visualize this induced polarization effect on P, we have considered the phosphoryl moiety derived from the two conformers **1b** and **1b′**, that is, we have deleted in both conformers the two apical substitutes. In the two resulting $PO(OH)_2$ moieties (one with the two HO opposite oriented and the other with the two HO parallel oriented) we have computed the molecular electrostatic potential (MEP), and the corresponding results are plotted in Figure 5. The phosphoryl having the two HO substitutes oppositely oriented, that derived from **1b**, (Figure 5a) has a symmetric distribution of the MEP in both sides of the equatorial plane, but, the phosphoryl group having the two HO substitutes parallel oriented, that derived from **1b′**, does not. Figure 5b,c

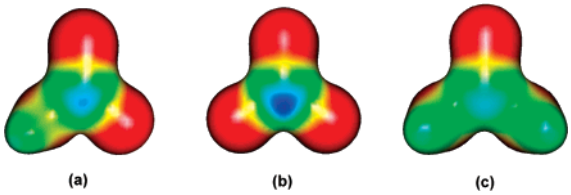

Figure 5. Molecular electrostatic potential representation of the $PO(OH)_2$ phosphoryl moiety of **1b** and **1b′** in a plane containing 98% of the electronic density: (a) one of the two symmetrical planes of **1b**; (b) opposite side of the equatorial hydrogens in **1b′**; and (c) side having the equatorial hydrogens in **1b′**.

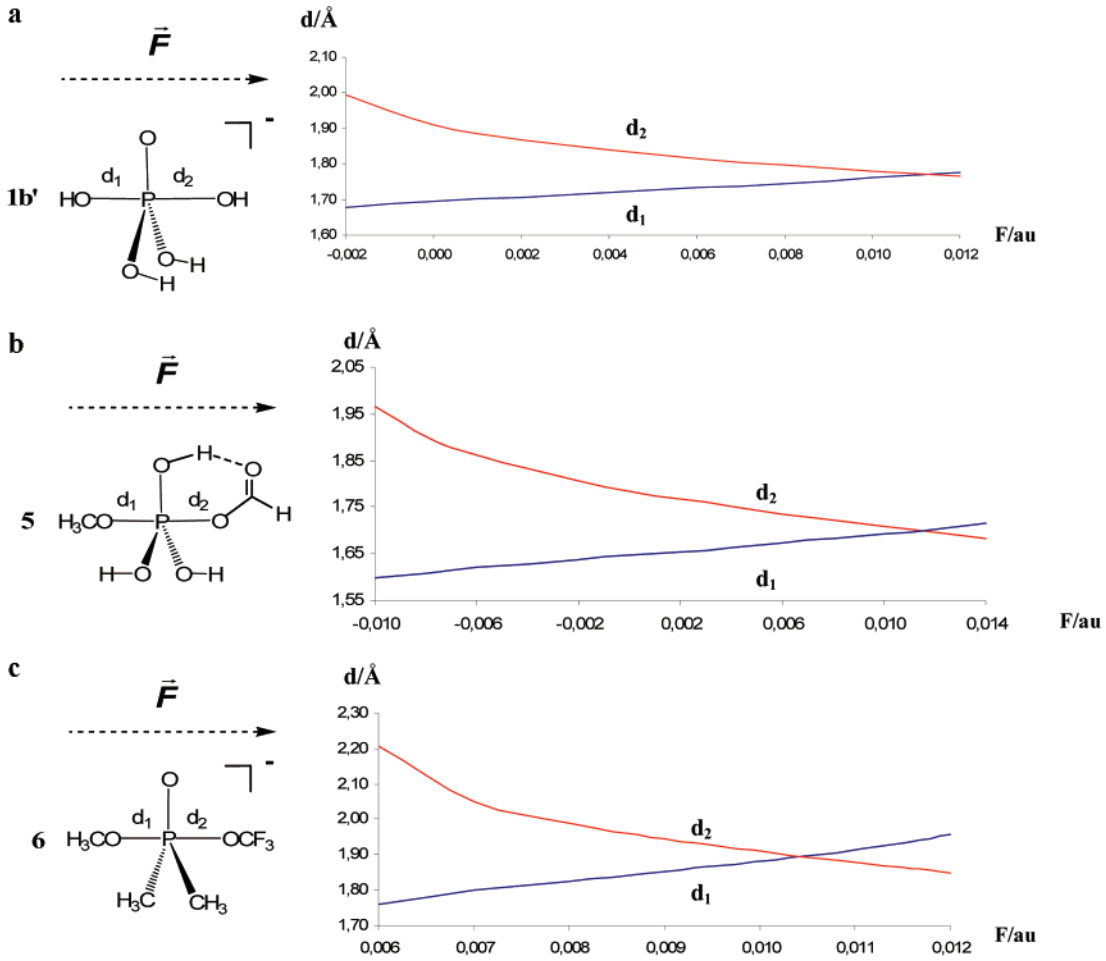

Figure 6. Dependence of the apical bond lengths on the intensity of an external electric field (*F*) for the pentacoordinated phosphorus compounds **1b′** (a), **5** (b), and **6** (c).

shows that it has a more positive charge density in the opposite side of the equatorial hydrogens. These results agree very much with the above discussion on **1b′**, where we have pointed out that a parallel orientation of the equatorial HO substitutes originates a large charge transfer to the side of the equatorial hydrogens (P1O6 bond in Figure 4).

A similar situation occurs with the compounds with equatorial substitutes CH_3O, structures **1c**−**3c**, and their corresponding conformers **1c′**−**3c′**. In a similar way as discussed above for **1b** and **1b′**, and as pointed out in the previous section, each pair of conformers differs at most by 3 kcal·mol^{-1}, being that the conformers **c** are more stable than the conformers **c′** (see Table 3). Figure 4 shows that compounds **1c**−**3c** have the CH_3O equatorial substitutes oppositely oriented and the two apical bond lengths equal (see also Table 1 and above), but a conformational change leading to the two equatorial substitutes parallel oriented (compounds **1c′**−**3c′**) produces, as just discussed for **1b** and **1b′**, a polarization effect on phosphorus that results in a significant change in the apical bond lengths. This is not so dramatic as for **1b** and **1b′**, because of the different electronegative character of the CH_3O equatorial substitutes, and the bond length changes induced amounts among 0.024 and 0.067 Å, depending on the apical substitutes (see Figure 4).

Effect of an External Electric Field. The high sensitivity to the polarization effects on the apical bonds, analyzed in the previous section, suggested to us to investigate the influence that an external electric field will produce on these kinds of bonds. To this end, we have performed a series of calculations on three pentacoordinated model systems and in two model reactions in order to analyze the effects of an external electric field on the geometries of the stationary point (minima) and on the reactivity. We have considered the effect of the external electric field in two different orientations, namely along a line in the plane defined by the phosphorus and the three equatorial substitutes and along the axis defined by the phosphorus and the apical substitutes. In the first case no substantial influence of the external electric field on the structures of the pentacoordinated models has been observed, but in the second case relevant effects have been found. Therefore, the results presented in this section correspond to the external electric field having the direction of the apical axis only. Putting the apical axis in the X direction and the origin of the coordinates at phosphorus, the external electric field follows the positive values of the X axis, while negative values means that the field direction was reversed. The results are displayed in Figures 6 and 7.

Regarding the influence of the electric field in the bonding and structural features, the first example we have considered

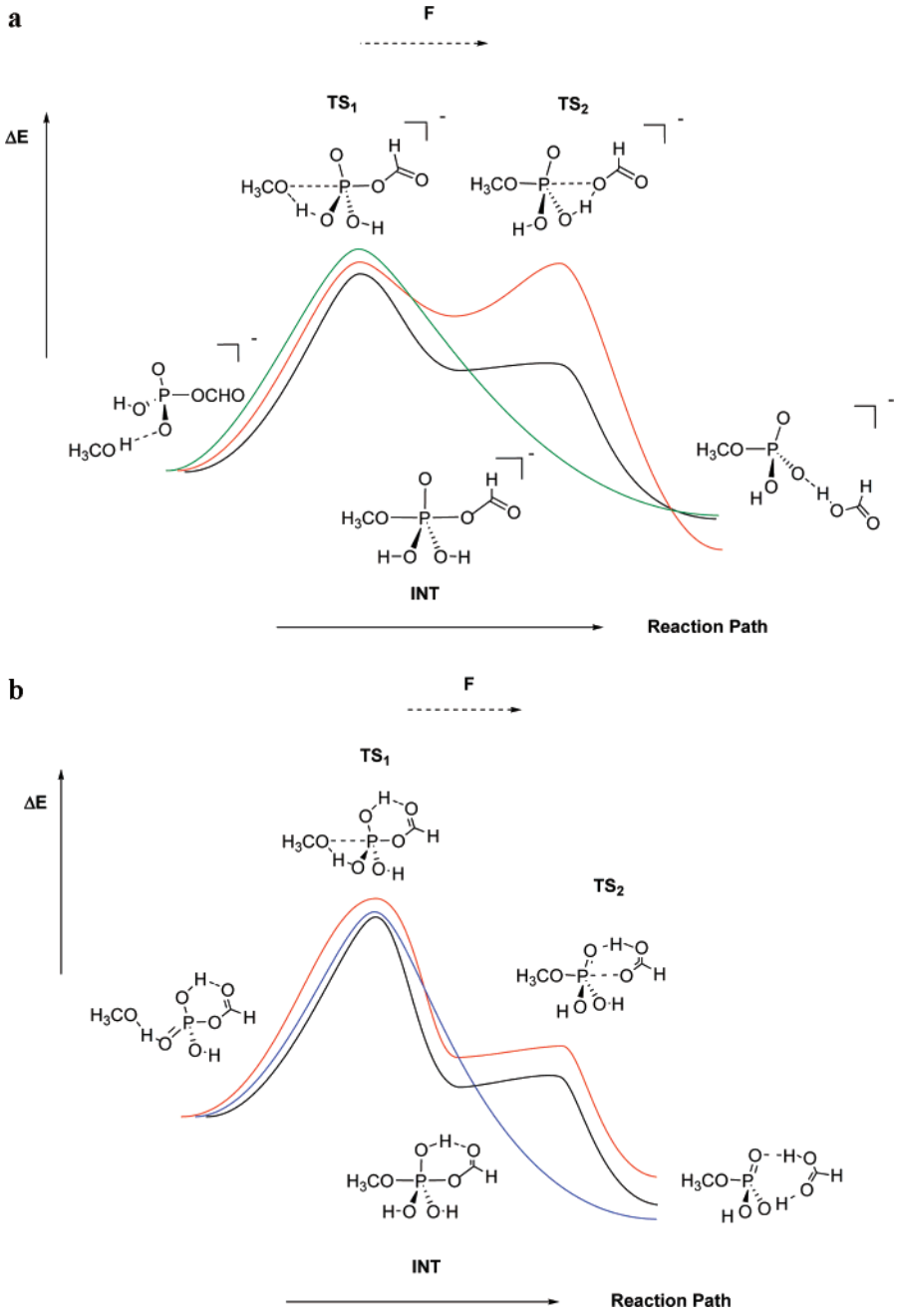

Figure 7. Schematic potential energy profiles computed under an external electric field at different intensities. (a) Corresponds to reaction 2 with $F = 0.0000$ au (black line); $F = 0.0060$ au (red line); and $F = -0.0020$ au (green line). (b) Corresponds to reaction 3 with $F = 0.0000$ au (black line); $F = 0.0060$ au (red line); and $F = -0.0060$ au (blue line).

is the model **1b′** ($PO(OH)_2(OH)_2$) discussed in the previous section and having the two equatorial OH substitutes parallel oriented (see Figure 4). We have pointed out that, in absence of external electric field, both apical P···O(H) bond lengths are different, 1.695 and 1.910 Å, respectively, for d_1 and d_2, but an external electric field produces important changes in these apical bond lengths. Figure 6a shows these changes as a function of the intensity of the external electric field. As the strength of F increases, d_1 is enlarged and d_2 is shortened so that applying an electric field of $F = 0.0111$ au both apical distances are equal, with a value of 1.769 Å. Figure 6a also shows that upon reversing the direction of the field, the opposite effect is observed, that is the d_2 is enlarged while d_1 is shortened, and with electric field with $F < -0.0030$ au, this pentacoordinated model is not stable anymore and dissociates in a process that involves a proton-transfer producing $H_2O + H_2PO_4^-$, as occurs in the process **1b** discussed in a previous section.

The second model we have considered under the effects of the electric field is $P(CH_3O)(HCOO)(HO)_3$ (compound **5**, see Figure 6b). This model is neutral, having three HO substitutes in an equatorial position, while the apical substitutes are CH_3O and HCOO. In the absence of an external electric field the two PO bond lengths are different (1.646 Å for P···OCH_3 and 1.785 Å for P···OCHO) as expected because, as pointed out above, the CH_3O apical substitute has a higher donor character. However, Figure 6b shows that the electric field produces a shortening of

the P···O(CHO) bond length and a lengthening of the P···O(CH_3) bond distance so that with an external electric field of $F = 0.0107$ au the two apical P···O bond distances become equal to 1.699 Å. Figure 6b also shows that with fields with $F > 0.0107$ au P···OCH_3 becomes larger than P···OCHO, which means that the electric field changes the relative strength of the two apical bonds.

The third model we have considered is PO(CH_3O)(OCF_3)-(CH_3)$_2$ having the two CH_3 as equatorial substitutes and OCH_3 and OCF_3 as apical substitutes (compound **6**, Figure 6c). This model has been chosen because in the absence of an external electric field, the pentacoordinated phosphorus compound is not stable and dissociates into PO(CH_3O)(CH_3)$_2$ and CF_3O^-. However, under a field of $F > 0.0060$ au, this pentacoordinated model is stable, being that the P···O(CH_3) bond length is shorter than the P···O(CF_3) until $F = 0.0105$ au, where both apical P···O bond distances become equal to 1.898 Å (see Figure 6c). When F increases beyond 0.0105 the P···O(CH_3) bond distance becomes larger than the P···O(CF_3) bond length, inverting thus the relative strength of the two apical bonds.

These three examples point out *a net influence of an external electric field on the bonding competence of the two apical dative bonds on phosphorus*.

With regard to the study of the effect of F on the reactivity we have considered the two following nucleophilic substitutions:

$$CH_3OH + POO(OH)(OCHO)^- \rightarrow POO(OH)(CH_3O)^- + HCOOH \quad (2)$$

$$CH_3OH + PO(OH)_2(OCHO) \rightarrow PO(OH)_2(CH_3O) + HCOOH \quad (3)$$

These two reactions differ in the fact that in the second one we have added a proton in order to have a neutral reaction. The results are displayed in Figure 7. In both cases the reaction begins with the formation of a prereactive hydrogen-bonded complex, whereas in the exit channel a hydrogen-bonded complex is also formed before the release of the products. As we are mainly interested in what concerns the pentacoordination at phosphorus, we will consider these hydrogen-bonded complexes as reactive products of reactions 2 and 3. Moreover, as for reactions **1b**−**4b** discussed above, these reactions involve, in the entry and exit channels, a proton transfer which is linked to the formation (breaking) of the pentacoordination at phosphorus. For reaction 2, Figure 7a shows that in the absence of an external electric field (black line), the pentacoordinated phosphorus intermediate **7** is computed to be 17.2 kcal·mol^{-1} higher in energy than the prereactive complex. Its formation (via **TS1**) requires the surmounting of an energy barrier of 34.3 kcal·mol^{-1}, whereas the energy barrier for the exit channel (**TS2**) is only 1.3 kcal·mol^{-1}, that is, **TS1** is clearly the limiting step of the reaction. Figure 7a shows also that the reaction profile is significantly altered under an external electric field. Thus, with a $F = 0.0060$ au (red line), the pentacoordinated intermediate **7** is destabilized by about 9 kcal·mol^{-1}, and, more interestingly, the computed energy barrier for the exit channel (**TS2**) is the same as that of the back reaction (**TS1**) to the reactants. On the other side, with an external field of $F = -0.0020$ au (green line), the pentacoordinated phosphorus intermediate is not stable anymore, and the reaction occurs in a single step. A similar behavior is observed for the neutral reaction 3 (Figure 7b). In the absence of an external electric field, the reaction occurs through the pentacoordinated intermediate **6** (black line) and is slightly destabilized when a $F = 0.0060$ au is applied (red line). However, with an $F = -0.0060$ au (blue line) the pentacoordinated intermediate is not stable anymore, and the reaction occurs in a single step. These two examples point out that *the external electric field affects the stability of pentacoordinated phosphorus compounds and it may also affect the reactivity of nucleophilic substitution at phosphorus*.

Scheme 2 [a]

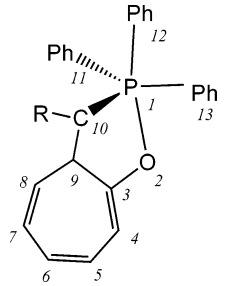

[a] **8a:** R = CH_3; **8b**: R = H; **8c**: R = CN.

These results may be of relevance in biological reactions involving pentacoordinated phosphorus, where the electric field originated by the folded protein could influence the catalytic process. In fact, it has been pointed out very recently the role of the electric field in the active site of the aldose reductase[76] and how the electric field may control the selectivity in heme enzymes.[77]

Triphenylphosphonium Ylide Derivatives. In an attempt to get a deeper insight in the hypervalence at phosphorus we have extended our investigation to the study on the bonding features of three neutral triphenylphosphonium ylide derivatives (**8**, Scheme 2) having pentacoordination at phosphorus and for which crystallographic X-ray data are available.[78,79]

These compounds have a trigonal bipyramid structure and are interesting for the purposes of this investigation because a change in the substitute R (R = CH_3 (**8a**), H (**8b**), and CN (**8c**)), which is not directly bonded to phosphorus, results in large changes in the P···O bond distance (2.00 Å for **8a**; 2.21 Å for **8b**; and 2.36 Å for **8c** (X-ray data)). The X-ray data first suggested that **8a** and **8b** form the PO bond but **8c** does not. Further analysis of the crystallographic data, together with results from ^{31}P and ^{13}C NMR spectra, had lead **8a**, **8b**, and **8c** to be viewed as resonance hybrids of structures A, B, and C (Scheme 3).[79,80] The δ_P and δ_C NMR spectra have been also collected in Table 4. **8a** shows a large δ_P (among −16.0 and −22.1 ppm, see also Table 4) that suggested a large contribution of the P−O bonding of the resonance structure A (Scheme 3). On the other hand, **8c** has a δ_P among −2.8 and −9.0 and has been related to the resonance structures B and C.

Scheme 3

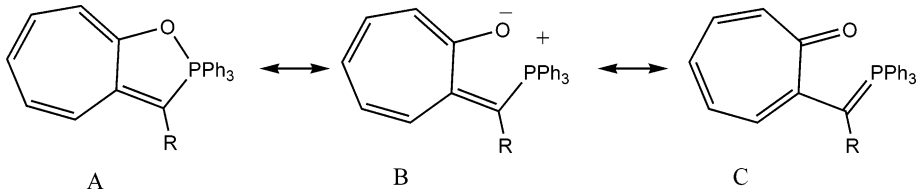

Table 4. Experimental and Computed ^{31}P and ^{13}C NMR Spectra (δ in ppm) for Compounds **8a**, **8b**, and **8c**[a]

	experimental values[69,70]					this work (gas phase)[b]		
	δ_P ($CDCl_3$)		δ_P (solid)	δ_C ($CDCl_3$)			δ_C	
compd	rt	−60 °C	rt	C3	C10	δ_P	C3	C10
8a	−17.9	−16.0	−22.1	170.1	87.0	−21.8	179.7	84.2
8b	−3.6	−1.8	−11.1	173.6	75.3	−16.2	180.2	77.8
8c	+7.8	+9.0	+2.8	177.5	49.4	−6.35	181.2	61.0

[a] Atom numbering is according to Scheme 2. [b] δ values are relative to H_3PO_4 for P and to TMS for C.

In the present work we have fully optimized and characterized as true minima the structures **8a**, **8b**, and **8c**, and their most significant geometrical parameters are displayed in Figure 8. It is gratifying to observe that the computed P···O bond distances compare well with the X-ray values for **8a** and **8b** (2.067 Å and 2.213 Å, respectively), whereas for **8c** our computed P···O bond length (2.239 Å) is 0.121 Å shorter than the X-ray value. Moreover, the remaining geometrical parameters compare also quite well with the experimental results. At this point, it should be taken into account that the calculated values should be compared with gas-phase values, while the X-ray data from the literature include packing effects that are shown to have an important role.[5,71] Besides the absolute values, the computed geometrical parameters follow the same trends with respect to the P···O bond lengths (**8a** < **8b** < **8c**). The bonding features have been analyzed, as above, employing the AIM and NBO methods, and the most significant results are displayed in the Supporting Information (Table S5). For each of the three triphenylphisphonium ylide considered (**8a**, **8b**, and **8c**), we have found a bcp between the phosphorus and oxygen atoms having the same topological features as those described in the previous sections for the P−O_{apical} bonds in the model systems, that is, the values of the density and the Laplacian of the density are small and positive, indicating that there is a *PO bond, that can be classified as dative*. Moreover, and as above, the NBO analysis indicates that the phosphorus has a formal sp^2 hybridization scheme. On the other hand, the large differences in the P···O bond distances observed for the three compounds, and originated by the different substitutes R, can be mainly associated with the different ability to delocalize the π system through the seven-member ring. Thus, **8c** with R = CN has a certain amount of π character between C and N, which prevents, in part, the delocalization of the π system through the C9−C10 bond. This results in a shorter CO bond distance with less ability to transfer charge to phosphorus, and consequently the P···O bond distance is larger. The opposite case **8a**, with R = CH_3, implies a different delocalization of the π system through the seven-member ring resulting in a larger CO bond distance with more ability to transfer charge from oxygen to phosphorus and consequently with a smaller P···O bond length. In any case, these results show that small changes in the electronic features produce large changes in the P···O bonding.

For the sake of completeness we have also computed the ^{31}P and ^{13}C NMR spectra of **8a**, **8b**, and **8c**, and the results have been collected in Table 4 along with the experimental data. The computed NMR spectra correspond to gas-phase

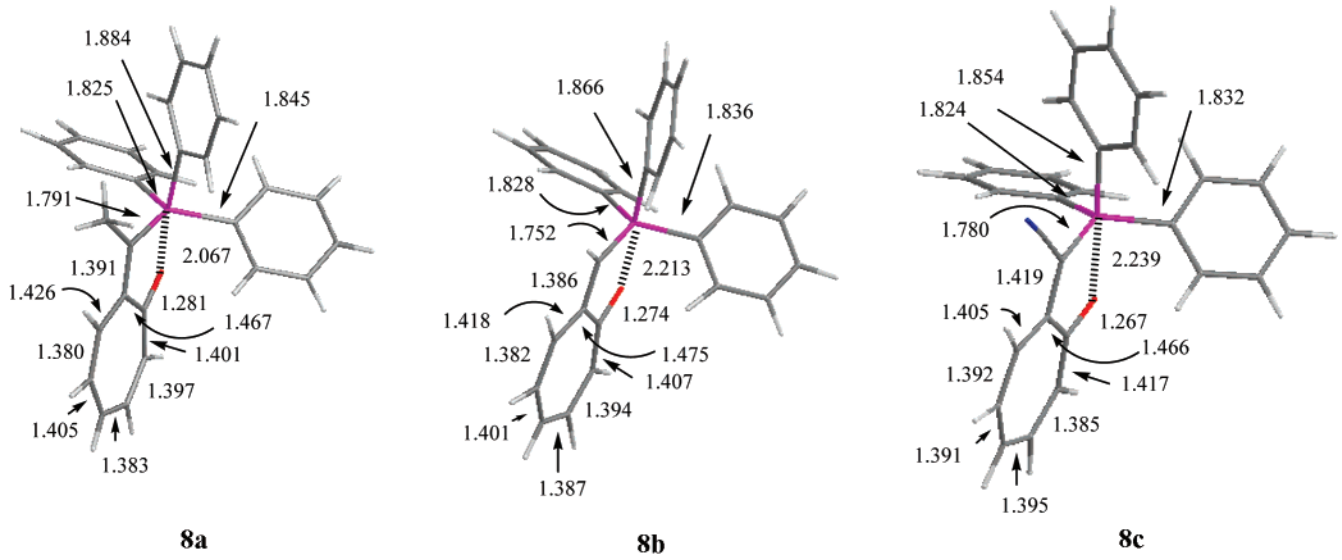

Figure 8. Selected geometrical parameters (in Å) for the optimized structures **8a**, **8b**, and **8c**. Atom numbering is according to Scheme 2.

optimized structures and show the same tendencies as the experimental values, that is larger δ_P for **8a** than for **8b** and for **8c** (−21.8, −16.2, and −6.35 ppm, respectively). Moreover, these results agree with the electronic features of the P←O dative bond. The stronger the P←O bond is, the higher the charge transfer associated with the dative bond and the shorter the corresponding bond length, which results in a higher shielding on P as reflected in the NMR spectra. It appears thus that the ^{31}P NMR spectra is a direct measure of the strength of dative bonding at phosphorus, and changes of its value in different media (as for instance in solid phase or in $CDCl_3$ for **8a**, **8b**, and **8c**, see refs 79 and 80 and also Table 4) would reflect differences in the bond length and strength. This also agrees with the linear correlation observed between δ_P and the X-ray P←O bond length as reported by Naya and Nitta.[79]

Conclusions

The results of the present investigation lead us to emphasize the following points: (1) All the pentacoordinated phosphorus compounds considered in this work have a trigonal bipyramid structure where the apical bonds show great variability. The topological and NBO analysis of the corresponding wave function indicates that these apical bonds can be classified as dative. These compounds are charge-transfer complexes, where the phosphorus has a formal sp^2 hybridization, which is compatible with the diagram based on a three-center four-electron (3c4e) model. (2) The features of the apical bonds depend strongly on the nature of the apical and equatorial substitutes. Compounds having apical substitutes with higher donor character are more stable and possess shorter apical bonds. On the other hand, the higher the donor character of the equatorial substitutes, the larger the apical bond length and the destabilization effect in pentacoordinated phosphorus compounds. (3) Polarization and electric field effects play an important role in the dative bonds of pentacoordinated phosphorus compounds, with consequences in both the geometry and the stability. These effects may change the competition between different apical substitutes, and they can even alter the reactivity of nucleophilic substitution at phosphorus. These effects may be of great relevance in enzymatic reactions, where the electric field originated by the folded protein could influence the catalytic process. (4) With regard to the three triphenylphosphonium ylide compounds considered (**8a**, **8b**, and **8c**), our results predict quite well the experimental (X-ray) geometrical data from the literature and show that in all cases there is a dative bond between the phosphorus and oxygen atoms, whose strength is correlated to the NMR displacement at P.

Acknowledgment. This research has been supported by the Generalitat de Catalunya (Grant 2005SGR00111). The calculations described in this work were carried out at the Centre de Supercomputació de Catalunya (CESCA) and at the Centro de Supercomputación de Galicia (CESGA), whose services are gratefully acknowledged. R.C. thanks also the Spanish Ramón y Cajal program.

Supporting Information Available: Cartesian coordinates of all structures reported in this paper and tables containing apical bond lengths for several model systems, optimized with different methods, activation and reaction energies for reaction **1b** obtained at different levels of theory, and AIM topological parameters for compounds **8**. This material is available free of charge via the Internet at http://pubs.acs.org.

References

(1) Skordalakes, E.; Dodson, G. G.; Green, D. S.; Goodwin, C. A.; Scully, M. F.; Hudson, H. R.; Kakkar, V. V.; Deadman, J. J. *J. Mol. Biol.* **2001**, *311*, 549−555.

(2) Lahiri, S. D.; Zhang, G. F.; Dunaway-Mariano, D.; Allen, K. N. *Science* **2003**, *299*, 2067−2071.

(3) Blackburn, G. M.; Williams, N. H.; Gamblin, S. J.; Smerdon, S. J. *Science* **2003**, *301*, 1184.

(4) Allen, K. N.; Dunaway-Mariano, D. *Science* **2003**, *301*.

(5) Holmes, R. R. *Acc. Chem. Res.* **2004**, *37*, 746−753.

(6) Leiros, I.; McSweeney, S.; Hough, E. *J. Mol. Biol.* **2004**, *339*, 805−820.

(7) Williams, N. H. *Biochim. Biophys. Acta* **2004**, *1697*, 279−287.

(8) Hengge, A. C.; Onyido, I. *Curr. Org. Chem.* **2005**, *9*, 61−74.

(9) Cleland, W. W.; Hengge, A. C. *Chem. Rev.* **2006**, *106*, 3252−3278.

(10) Wittinghofer, A. *Trends. Biochem. Sci.* **2006**, *31*, 20−23.

(11) Swamy, K. C.; Kumar, N. S. *Acc. Chem. Res.* **2006**, *39*, 324−333.

(12) Catrina, I.; O'Brien, P. J.; Purcell, J.; Nikolic-Hughes, I.; Zalatan, J. G.; Hengge, A. C.; Herschlag, D. *J. Am. Chem. Soc.* **2007**, *129*, 5760−5765.

(13) Mildvan, A. S. *Proteins* **1997**, *29*, 401−416.

(14) Allen, K. N.; Dunaway-Mariano, D. *Trends. Biochem. Sci.* **2004**, *29*, 495−503.

(15) Vedejs, E.; Marth, C. F. *J. Am. Chem. Soc.* **1988**, *110*, 3948−3958.

(16) Tremblay, L. W.; Zhang, G. F.; Dai, J. Y.; Dunaway-Mariano, D.; Allen, K. N. *J. Am. Chem. Soc.* **2005**, *127*, 5298−5299.

(17) Godfrey, S. M.; McAuliffe, C. A.; Pritchard, R. G.; Sheffield, J. M. *Chem. Commun.* **1998**, 921−922.

(18) Chandrasekaran, A.; Timosheva, N. V.; Day, R. O.; Holmes, R. R. *Inorg. Chem.* **2003**, *42*, 3285−3292.

(19) Hu, C. H.; Brinck, T. *J. Phys. Chem. A* **1999**, *103*, 5379−5386.

(20) Bianciotto, M.; Barthelat, J. C.; Vigroux, A. *J. Phys. Chem. A* **2002**, *106*, 6521−6526.

(21) Berente, I.; Beke, T.; Náray-Szabó, G. *Theor. Chem. Acc.* **2007**, *118*, 129−134.

(22) Wang, Y. N.; Topol, I. A.; Collins, J. R.; Burt, S. K. *J. Am. Chem. Soc.* **2003**, *125*, 13265−13273.

(23) Pepi, F.; Ricci, A.; Rosi, M.; Di Stefano, M. *Chem.-Eur. J.* **2004**, *10*, 5706−5716.

(24) Van Bochove, M. A.; Swart, M.; Bickelhaupt, F. M. *J. Am. Chem. Soc.* **2006**, *128*, 10738−10744.

(25) Lopez, X.; Schaefer, M.; Dejaegere, A.; Karplus, M. *J. Am. Chem. Soc.* **2002**, *124*, 5010−5018.

(26) Lopez, X.; York, D. M.; Dejaegere, A.; Karplus, M. *Int. J. Quantum Chem.* **2002**, *86*, 10−26.

(27) Lopez, X.; Dejaegere, A.; Leclerc, F.; York, D. M.; Karplus, M. *J. Phys. Chem. B* **2006**, *110*, 11525−11539.

(28) Imhof, P.; Fischer, S.; Kramer, R.; Smith, J. C. *J. Mol. Struct. (THEOCHEM)* **2005**, *713*, 1−5.

(29) Grzyska, P. K.; Czyryca, P. G.; Golightly, J.; Small, K.; Larsen, P.; Hoff, R. H.; Hengge, A. C. *J. Org. Chem.* **2002**, *67*, 1214−1220.

(30) Chen, S. L.; Fang, W. H.; Himo, F. *J. Phys. Chem. B* **2007**, *111*, 1253−1255.

(31) Klahn, M.; Rosta, E.; Warshel, A. *J. Am. Chem. Soc.* **2006**, *128*, 15310−15323.

(32) Iche-Tarrat, N.; Ruiz-Lopez, M.; Barthelat, J. C.; Vigroux, A. *Chem.-Eur. J.* **2007**, *13*, 3617−3629.

(33) Cramer, C. J.; Gustafson, S. M. *J. Am. Chem. Soc.* **1993**, *115*, 9315−9316.

(34) Seckute, J.; Menke, J. L.; Emnett, R. J.; Patterson, E. V.; Cramer, C. J. *J. Org. Chem.* **2005**, *70*, 8649−8660.

(35) Uchimaru, T.; Tanabe, K.; Nishikawa, S.; Taira, K. *J. Am. Chem. Soc.* **1991**, *113*, 4351−4353.

(36) Yliniemela, A.; Uchimaru, T.; Tanabe, K.; Taira, K. *J. Am. Chem. Soc.* **1993**, *115*, 3032−3033.

(37) Tole, P.; Lim, C. M. *J. Phys. Chem.* **1993**, *97*, 6212−6219.

(38) Lim, C.; Tole, P. *J. Phys. Chem.* **1992**, *96*, 5217−5219.

(39) Lim, C.; Tole, P. *J. Am. Chem. Soc.* **1992**, *114*, 7245−7252.

(40) Chang, N. Y.; Lim, C. *J. Phys. Chem. A* **1997**, *101*, 8706−8713.

(41) Chang, N. Y.; Lim, C. *J. Am. Chem. Soc.* **1998**, *120*, 2156−2167.

(42) Dudev, T.; Lim, C. *J. Am. Chem. Soc.* **1998**, *120*, 4450−4458.

(43) Zhou, D. M.; Taira, K. *Chem. Rev.* **1998**, *98*, 991−1026.

(44) Taira, K.; Uchimaru, T.; Storer, J. W.; Yliniemela, A.; Uebayasi, M.; Tanabe, K. *J. Org. Chem.* **1993**, *58*, 3009−3017.

(45) Uchimaru, T.; Tsuzuki, S.; Storer, J. W.; Tanabe, K.; Taira, K. *J. Org. Chem.* **1994**, *59*, 1835−1843.

(46) Uchimaru, T.; Stec, W. J.; Tsuzuki, S.; Hirose, T.; Tanabe, K.; Taira, K. *Chem. Phys. Lett.* **1996**, *263*, 691−696.

(47) Range, K.; McGrath, M. J.; Lopez, X.; York, D. M. *J. Am. Chem. Soc.* **2004**, *126*, 1654−1665.

(48) Adamo, C.; Barone, V. *J. Chem. Phys.* **1998**, *108*, 664−675.

(49) Hariharan, P. C.; Pople, J. A. *Theor. Chim. Acta* **1973**, *28*, 213.

(50) Gilbert, T. M. *J. Phys. Chem. A* **2004**, *108*, 2550−2554.

(51) Moeller, C.; Plesset, M. S. *Phys. Rev.* **1934**, *46*, 618.

(52) Frisch, M. J.; Head-Gordon, M.; Pople, J. A. *Chem. Phys. Lett.* **1990**, *166*, 281.

(53) Head-Gordon, M.; Head-Gordon, T. *Chem. Phys. Lett.* **1994**, *220*, 122.

(54) Ishida, K.; Morokuma, K.; Kormornicki, A. *J. Chem. Phys.* **1977**, *66*, 2153.

(55) Gonzalez, C.; Schlegel, H. B. *J. Chem. Phys.* **1989**, *90*, 2154.

(56) Gonzalez, C.; Schlegel, H. B. *J. Phys. Chem.* **1990**, *94*, 5523.

(57) Krishnan, R.; Binkley, J. S.; Seeger, R.; Pople, J. A. *J. Chem. Phys.* **1980**, *72*, 650.

(58) Cizek, J. *Adv. Chem. Phys.* **1969**, *14*, 35.

(59) Barlett, R. J. *J. Phys. Chem.* **1989**, *93*, 1963.

(60) Pople, J. A.; Krishnan, R.; Schlegel, H. B.; Binkley, J. S. *Int. J. Quantum Chem. XIV* **1978**, 545−560.

(61) Truhlar, D. G. *Chem. Phys. Lett* **1998**, *294*, 45−48.

(62) Fast, P. L.; Sanchez, M. L.; Truhlar, D. G. *J. Chem. Phys.* **1999**, *111*, 2921−2926.

(63) Becke, A. D. *J. Chem. Phys.* **1993**, *98*, 5648.

(64) Cheeseman, J. R.; Trucks, G. W.; Keith, T. A.; Frisch, M. F. *C. J. Chem. Phys.* **1996**, *104*, 5497−5509.

(65) Wolinski, K.; Hinton, J. F.; Pulay, P. *J. Am. Chem. Soc.* **1990**, *112*, 8251−8260.

(66) Frisch, M. J.; Trucks, G. W.; Schlegel, H. B.; Scuseria, G. E.; Robb, M. A.; Cheeseman, J. R. J. A.; Montgomery, J.; Vreven, T.; Kudin, K. N.; Burant, J. C.; Millam, J. M.; Iyengar, S. S.; Tomasi, J.; Barone, V.; Mennucci, B.; Cossi, M.; Scalmani, G.; Rega, N.; Petersson, G. A.; Nakatsuji, H.; Hada, M.; Ehara, M.; Toyota, K.; Fukuda, R.; Hasegawa, J.; Ishida, M.; Nakajima, T.; Honda, Y.; Kitao, O.; Nakai, H.; Klene, M.; Li, X.; Knox, J. E.; Hratchian, H. P.; Cross, J. B.; Adamo, C.; Jaramillo, J.; Gomperts, R.; Stratmann, R. E.; Yazyev, O.; Austin, A. J.; Cammi, R.; Pomelli, C.; Ochersk i, J. W.; Ayala, P. Y.; Morokuma, K.; Voth, G. A.; Salvador, P.; Dannenberg, J. J.; Zakrzewski, V. G.; Dapprich, S.; Daniels, A. D.; Strain, M. C.; Farkas, O.; Malick, D. K.; Rabuck, A. D.; Raghavachari, K.; Foresman, J. B.; Ortiz, J. V.; Cui, Q.; Baboul, A. G.; Clifford, S.; Cioslowski, J.; Stefanov, B. B.; Liu, G.; Liashenko, A.; Piskorz, P.; Komaromi, I.; Martin, R. L.; Fox, D. J.; Keith, T.; Al-Laham, M. A.; Peng, C. Y.; Nanayakkara, A.; Challacombe, M.; Gill, P. M. W.; Johnson, B.; Chen, W.; Wong, M. W.; Gonzalez, C.; Pople, J. A. *Gaussian 03, Revision C.01*; Gaussian, Inc.: Wallingford, CT, 2004.

(67) Shaftenaar, G.; Noordik, J. H. *J. Comput.-Aided Mol. Des.* **2000**, *14*, 123−134.

(68) Reed, A. E.; Curtiss, L. A.; Weinhold, F. *Chem. Rev.* **1988**, *88*, 899−926.

(69) Bader, R. F. W. *Atoms in Molecules. A Quantum theory*; Clarendon Press: Oxford, 1995; Vol. 22, pp 1−458

(70) Bader, R. F. W. *AIMPAC*. http://www.chemistry.mcmaster.ca/aimpac (accessed May 2002)

(71) Leopold, K. R.; Canagaratna, M.; Phillips, J. A. *Acc. Chem. Res.* **1997**, *30*, 57−64.

(72) Anglada, J. M.; Bo, C.; Bofill, J. M.; Crehuet, R.; Poblet, J. M. *Organometallics* **1999**, *18*, 5584−5593.

(73) Reed, A. E.; Schleyer, P. V. *J. Am. Chem. Soc.* **1990**, *112*, 1434−1445.

(74) Massey, A. G. In *Main Group Chemistry*; John Wiley and Sons: Chichester, England, 2000.

(75) Bento, A. P.; Bickelhaupt, F. M. *J. Org. Chem.* **2007**, *72*, 2201−2207.

(76) Suydam, I. T.; Snow, C. D.; Pande, V. S.; Boxer, S. G. *Science* **2006**, *313*, 200−204.

(77) Shaik, S.; de Visser, S. P.; Kumar, D. *J. Am. Chem. Soc.* **2004**, *126*, 11746−11749.

(78) Kawamoto, I.; Hata, T.; Kishida, Y.; Tamura, C. *Tetrahedron Lett.* **1971**, 2417-&.

(79) Naya, S.; Nitta, M. *J. Chem. Soc., Perkin Trans.* **2002**, *2*, 1017−1023.

(80) Nitta, M.; Naya, S. *J. Chem. Res.-S* **1998**, 522−523.

CT700220Z